

6. CORRELATION OF HIGH-RESOLUTION SEISMIC DATA WITH ODP LEG 208 BOREHOLE MEASUREMENTS¹

Thomas Bartels,² Sebastian Krastel,² and Volkhard Spiess²

ABSTRACT

Walvis Ridge, located in the eastern South Atlantic Ocean, is one of the few known locations where it is possible to recover undisturbed, complete, and possibly expanded Paleogene sediments over a wide range of water depths. The main objective of Ocean Drilling Program (ODP) Leg 208, realized on outer Walvis Ridge in the summer of 2003, was recovery of intact composite sequences of “critical” transitions like the Cretaceous/Tertiary (K/T) boundary, Eocene/Oligocene (E/O) boundary, Paleocene/Eocene Thermal Maximum (PETM), and the Elmo event.

Meteor Cruise M49/1, in early 2001, was the main seismic presite survey for Leg 208. The high-resolution multichannel seismic system of the University of Bremen was used to identify drill sites at outer Walvis Ridge that promised recovery of undisturbed, complete, and possibly expanded Cenozoic sequences. Based on these new seismic data, six sites were drilled at water depths between 2500 and 4755 m on the northeastern flank of Walvis Ridge during Leg 208.

To ground truth the seismic record, synthetic seismograms were calculated from closely spaced core logging density measurements of Leg 208 cores. The high quality of both seismic and core logging data allows good correlation between synthetic seismograms and recorded seismic data. These results allow identification and characterization of target reflection horizons like the E/O boundary, Elmo horizon, PETM, and K/T boundary in seismic images and dating of individual reflectors.

Total sediment thickness in the survey area varies between 200 and 530 m, and the study area can be separated into three zones that have

¹Bartels, T., Krastel, S., and Spiess, V., 2007. Correlation of high-resolution seismic data with ODP Leg 208 borehole measurements. *In* Kroon, D., Zachos, J.C., and Richter, C. (Eds.), *Proc. ODP, Sci. Results*, 208: College Station, TX (Ocean Drilling Program), 1–27. doi:10.2973/odp.proc.sr.208.204.2007

²Department of Geosciences, University Bremen, PO Box 330440, D-288334 Bremen, Germany. Correspondence author: bartelst@uni-bremen.de

Initial receipt: 5 September 2005

Acceptance: 28 February 2007

Web publication: 17 April 2007

Ms 208SR-204

different deposition conditions. In general, seismic data show a decrease in total sediment thickness with increasing distance from the ridge crest, but lateral variations in sedimentation rates were found across the entire survey area. Especially close to the crest of the ridge, these lateral variations in sedimentation rates might indicate the influence of bottom water currents on sedimentation at the outer Walvis Ridge.

INTRODUCTION

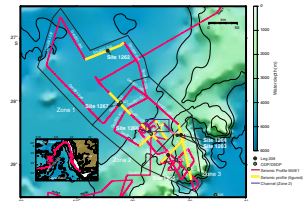
Walvis Ridge is a northeast-southwest-trending aseismic ridge that effectively divides the eastern South Atlantic Ocean into two basins: Angola Basin to the north and Cape Basin to the south (Fig. F1). The ridge consists of a series of interconnected crustal blocks that slope gradually toward the northwest and more steeply toward the southeast. Magnetic and gravity anomalies indicate that the ridge was formed by hotspot volcanism near the mid-ocean ridge as the basin gradually widened (Rabinowitz and Simpson, 1984). Walvis Ridge is well known as a nearly impassable barrier for bottom waters (Arhan et al., 2003). Pelagic sediments drape most of the ridge and generally increase in thickness toward the continental margin (Moore, Rabinowitz, et al., 1984). It is assumed that the ridge followed a simple thermal subsidence of ~1.1 km since the Maastrichtian (Moore, Rabinowitz, et al., 1984).

The thickness of pelagic sediments varies from ~200 m on the deep (>4.5 km) seafloor adjacent to the ridge to ~530 m near the summit (~2.5 km). These sediments are primarily calcareous oozes and chalks that range in age from Campanian to Holocene. In the Neogene section, nannofossil and foraminiferal nannofossil oozes with relatively high carbonate contents of as much as 90 wt% were found. The lower to middle Miocene sections are characterized by lower carbonate values between 0 and 20 wt%. Some intercalated slumps and turbidites were identified in Neogene deposits. Paleogene sediments are dominated by nannofossil- and foraminifer-bearing nannofossil oozes to chalk. The sediments have high carbonate contents, up to 80 wt%, through most of the Paleocene, Eocene, and Oligocene. Some smaller carbonate-poor intervals indicate episodes of carbonate compensation depth (CCD) shoaling (Zachos, Kroon, Blum, et al., 2004).

In spring 2003, six sites were drilled on outer Walvis Ridge during Ocean Drilling Program (ODP) Leg 208. The main objectives of Leg 208 were to analyze extreme climatic conditions in the Paleogene, date and utilize astronomical cycles, and reconstruct the eastern equatorial paleo-oceanographic development. *Meteor* Cruise M49/1 in early 2001 acted as main seismic presite survey for Leg 208 to optimize drill site locations.

To ground truth seismic records and to construct a more precise seismic stratigraphy, it is possible to correlate seismic records with well data from a nearby drill site by modeling reflection patterns. This was accomplished by visual correlation of seismic traces with synthetic seismograms, calculated from drill site density and velocity measurements (e.g., Zühlsdorff and Spiess, 2001; White and Hu, 1998). The best results are commonly achieved when downhole logging data from near-vertical wells are available (White and Hu, 1998), but if, as in this study, no downhole velocity log exists, it is possible to estimate sonic data from density logs (e.g., Adcock, 1993; Zühlsdorff and Spiess, 2001). Therefore velocity and density profiles were constructed from measurements on rock samples or from core logging data as provided by the gamma ray

F1. Seismic presite survey, p. 13.



attenuation (GRA) densitometer and the *P*-wave logger (PWL). Correlation of seismic data collected during *Meteor* Cruise M49/1 and core logging data measured during Leg 208 is a very promising approach because of the high quality of both data sets. In this paper we present seismic data from the presite survey collected during *Meteor* Cruise M49/1 and identify the target horizons of Leg 208 sites using synthetic seismograms. Using the stratigraphy of Leg 208 cores (Shipboard Scientific Party, 2003), this method permits assignment of ages to individual reflectors and characterization of the seismic signature of target horizons. Seismic data will also be used for a first investigation of sedimentary features at outer Walvis Ridge.

DATA AND METHODS

Seismic Data

Meteor Cruise M 49/1 in early 2001 from Cape Town (South Africa) to Montevideo (Uruguay) was the main presite survey for Leg 208. The main objectives were to collect high-resolution seismic reflection profiles to identify drill sites that promise recovery of undisturbed, complete, and possibly expanded Paleogene sequences in different water depths. Seismic profiles with a total length of ~1800 were acquired in the study area in water depths between ~2.5 and 4.5 km (Fig. F1).

The multichannel seismic system of the University of Bremen is specifically designed to collect seismic data with high lateral and vertical resolution. The alternating operation of a small-chamber water gun (0.16 L; 200–1600 Hz), a generator-injector (GI) gun with reduced chamber volume (0.4 L; 100–500 Hz), and a GI gun with normal chamber volume (1.7 L; 30–200 Hz) yielded three seismic data sets simultaneously. For recording of the GI gun and water gun data, a 96-channel Syntron streamer 600 m in length and equipped with separately programmable hydrophone groups was used. In this manuscript, we will only present GI gun data. A total of 48 channels consisting of 13 hydrophones each, a group length of 6.25 m, and a group distance of 12.5 m were used for recording GI gun data. The shot interval was 9 s, resulting in a shot distance of ~25 m when sailing with an average speed of 6 kt. Ten birds kept the streamer at a constant water depth of ~3 m below the sea surface within a range of 1 m. A magnetic compass at every bird allowed determination of hydrophone group position relative to the ship's course. GI gun data were digitally recorded at a sampling frequency of 4 kHz over a record length of 3000 ms. Positioning was based on Global Positioning System (GPS). For processing of seismic data a combination of in-house and commercial (Vista) software (Seismic Image Software LTD) was used. Standard seismic processing procedures employed included trace editing, setting up geometry, static and delay corrections, velocity analysis, normal move-out (NMO) corrections, bandpass frequency filtering, stacking, and time migration. A common midpoint (CMP) distance of 10 m was chosen for processing.

Calculation of Synthetic Seismograms

The reflection coefficient (*R*) between media of densities ρ_1 and ρ_2 and velocities v_1 and v_2 is given for vertical incidence waves by the Zoepritz equation:

$$R = [(\rho_1 \cdot v_1) - (\rho_2 \cdot v_2)] / [(\rho_1 \cdot v_1) + (\rho_2 \cdot v_2)].$$

The sequence of velocity and density changes with depth below the seafloor is referred to as Earth's reflection coefficient series. This series can be transformed into two-way traveltime (TWT) scale using velocity measurements. The synthetic seismogram can be calculated by mathematically convolving this series with the seismic wavelet. The impulse response function for seismic modeling was computed using the state space approach (Mendel et al., 1979), which also takes all possible internal reflections into account. By comparing reflectors in the synthetic seismogram with core density measurements, it is possible to assign reflectors to geologic events. The detailed procedure for calculating the synthetic seismogram is described below.

Editing of GRA Density Data

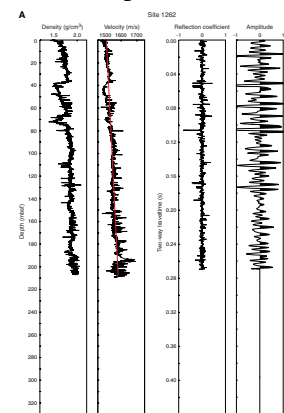
GRA density measurements with a sampling interval of 2 to 3 cm are available for all Leg 208 sites. All sites consist of two to four holes. As individual holes usually do not recover the entire stratigraphy of a site, it is necessary to merge and edit the density data to create composite data sets for each site (Fig. F2A, F2B). This was done using stratigraphic tie points determined during the cruise (Shipboard Scientific Party, 2003).

After creating a composite data set for each site, a moving window with a length of 50 measured values was used to calculate a local average density and to detect spurious density values, likely caused by voids, cracks, or gas bubbles within the cores and at the ends of the core sections. These artifacts cause unrealistic values for reflection coefficients and thus are replaced by the last density value accepted by the moving window. The criterion to replace was that a value should not differ more than four times the root mean square deviation of the window. Furthermore, data gaps that could not be filled were linearly interpolated to avoid unnatural reflection coefficients caused by small data gaps. A correction of the GRA density values to in situ conditions, which accounts for decrease in hydrostatic pressure, temperature change, and porosity rebound during core recovery (Hamilton, 1976), was not carried out because relative density variations especially for the upper 150 m of the sediment column will not be significantly changed (e.g., Mosher et al., 1993; Rohr and Gröschel-Becker, 1994).

P-Wave Velocity Models

Sampling intervals of whole-core velocity data sets are ~25 cm and more, which is much larger than the sampling intervals of the GRA density measurements of Leg 208 cores (Shipboard Scientific Party, 2003). This discrepancy makes it impossible to calculate reflection coefficients with a detailed velocity model. Additionally, detailed velocity measurements were not done at all depths of each site. Adventitious velocity data are less important for the calculation of reflection coefficients because values scatter around a mean trend and variations in marine surface sediments do not exceed 5% (e.g., Weber et al., 1997; Breitzke, 2000). In contrast, associated density variations within marine surface sediments are usually >20% (e.g., Weber et al., 1997; Breitzke, 2000). A careful analysis of velocity and GRA density measurements shows a positive correlation of smaller velocity excursions and density variations. Therefore, the effect of the velocity data on the reflection coefficient is small. We estimate the overall error, which is introduced by

F2. Core data, p. 14.



assuming a smooth velocity depth profile and ignoring the velocity contribution to variations in reflection coefficients, to be only 10%–20%. Zühlsdorff and Spiess (2001) estimated similar errors using the same methods for data from ODP Leg 168 at the eastern flank of Juan de Fuca Ridge.

Close inspection of velocity data also shows a large number of spurious data points. These facts support the use of a simple velocity model that is still sufficient to identify our target reflectors but with obvious restrictions. For example, interpretation of waveforms, as well as interpretation of amplitudes of individual reflectors, is of limited quality because effects such as interference definitely cause discrepancies between recorded and modeled data.

The velocity model is, of course, also needed for conversion of the meters below seafloor scale to a timescale.

Correlation of Synthetic Seismograms with the Seismic Record

After creating whole continuous GRA density data sets for each site, it is necessary to convert the meters below seafloor scale to a timescale and to calculate the series of reflection coefficients. In the first step, a constant velocity of 1500 m/s was used. A sampling interval of 250 μ s, which is the same as for seismic data, was used to preserve complete information for GRA density measurements. To create a seismic trace, density data must be convolved using a seismic wavelet. Although it is possible to pick seafloor reflections, a synthetic wavelet is used. Synthetic wavelets are smoother than recorded wavelets and appear to be more useful for visual correlation of reflection patterns. Differences in vertical energy distribution between synthetic wavelets and recorded wavelets do not appear (Zühlsdorff and Spiess, 2001). In this study, for convolving reflection coefficients, a Ricker wavelet (Ricker, 1953) with a frequency of 150 Hz, which is the main frequency of the GI gun, was used (Fig. F2A, F2B, F2C, F2D). Synthetic data were then compared with seismic data at the CMP of the drill site location. In the next step, the velocity model was fine tuned using velocity information from whole-core analysis to improve depth to time conversion for better synthetic to seismic matching. It turned out that the best-fit velocity models usually correspond to linear regressions of velocity measurements, which take the general velocity trend into account, namely the increase of the velocity with depth, but neglect all small-scale velocity variations (Fig. F2A, F2B, F2C, F2D).

For Site 1267 no velocity measurements or information exist; therefore, a velocity model of a nearby drill site is used. In this case, the velocity model of Site 1266 is used; Site 1266 is located on the same seismic profile, GeoB01-030, which is characterized by only few changes in the sedimentation pattern.

DESCRIPTION OF SITES

Six sites were drilled at water depths between 2500 and 4770 m on the northeastern flank of Walvis Ridge during Leg 208 (Fig. F1). The main objective of Leg 208 was to recover intact composite sequences of “critical” transitions in the Paleogene (Shipboard Scientific Party, 2003). This paper concentrates on these transitions, namely the following:

1. Eocene/Oligocene (E/O) boundary (35.7 Ma): this sharp transition is marked by a step increase in magnetic measurements and a step decrease in color lightness (Shipboard Scientific Party, 2003).
2. Chron C24n Elmo event (53.2 Ma): this event is characterized by a drop in calcium carbonate content in the sediment (Scientific Shipboard Party, 2003) and is characterized by a density contrast of ~10% in comparison to the surrounding sediments. The layer was reached at five of the six sites and has a thickness of ~30 cm (Shipboard Scientific Party, 2003).
3. Paleocene/Eocene Thermal Maximum (PETM, 55 Ma): isotope records suggest that at ~55 Ma the deep ocean and high-latitude surface waters warmed by 4°C and 8°C, respectively (e.g., Kaiho et al., 1996). The PETM at Leg 208 sites is a clay layer without carbonate content. The thickness of the layer varies from 50 cm at the deepest site to 80 cm at shallower sites. Like the Elmo horizon, the density of the PETM increases ~10% (Shipboard Scientific Party, 2003).

Additionally, it is possible to identify the Miocene *Bolivina* Acme event (18 Ma), which represents a foraminiferal assemblage dominated by small, smooth, thin-walled bolivinids (Smart and Murray, 1994), at all sites and the Cretaceous/Tertiary (K/T) boundary (66.4 Ma) at the two deepest sites, Sites 1262 and 1267.

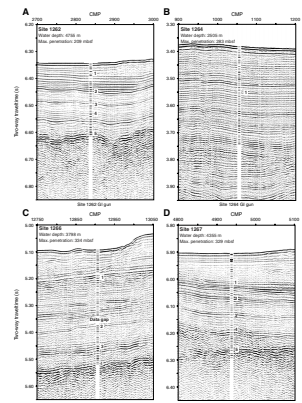
Identification of critical transitions on seismic data was done by correlating the synthetic seismograms. Figure F3 shows data examples for Sites 1262, 1264, 1266, and 1267. Because of the high quality of both data sets, the reflection patterns of the synthetic seismograms fit well with the seismic traces. This “event modeling” offers the possibility to assign characteristic layers of the drill sites to seismic reflectors. The depth values of the target horizons described below are calculated from seismic traveltime, including the simplified linear velocity model used for calculation of synthetic seismograms. Scaling the resolution of the top and base of the target horizons (such as the PETM and Elmo) on a meter to submeter scale is not possible with a GI gun (~150 Hz) as a seismic source. For this task a wavelet with a length not smaller than two times the thickness of the layer is needed (Badley, 1985). However, the fit of the reflection pattern, together with the knowledge of the physical properties of each event (Scientific Shipboard Party, 2003), allows identification of seismic reflectors in which each event must be included. Because of changing density values (e.g., the increase of 10% for the Elmo horizon and the PETM), those reflectors are mostly characterized by stronger amplitudes.

Synthetic seismograms for Sites 1263 and 1265 are missing because of spurious data values in the GRA density values, where synthetic seismograms do not fit with the seismic data. Hence, identification of target horizons at both sites is based on correlation between Leg 208 sites by tracing the target horizons along the seismic profiles. Table T1 summarizes depths of the target horizons for each Leg 208 site.

Site 1262

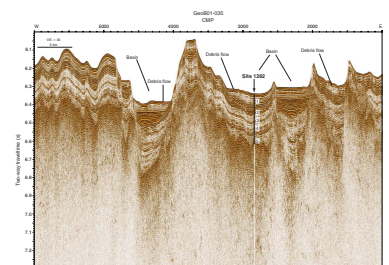
Site 1262 (Fig. F4), located on Profile GeoB01-035 at a water depth of ~4755 m, is the deepest site of the drilling transect, situated at the edge of Angola Basin. The seismic profile is characterized by an undulating topography with a number of sedimentary ridges located on top of

F3. Synthetic seismograms and seismic data, p. 18.



T1. Depth of target horizons, p. 27.

F4. Seismic Line GeoB01-035, Site 1262, p. 19.



basement highs and small sedimentary basins in between. Several debris flows and/or slumps were imaged as transparent zones in the sedimentary basins. Total sediment thickness is between 150 and 220 m (Fig. F4). Site 1262 is located in one of the small sedimentary basins. The upper ~100 ms TWT is characterized by continuous reflectors with high amplitudes. A debris flow or slump is located in this depth interval directly west of the site. The upper ~100 ms TWT represents Neogene and Eocene sediments. The Miocene *Bolivina* Acme event is found in this interval at ~53 mbsf and can be characterized by a reflector with high amplitudes. At the depth of ~100 ms TWT, the seismic pattern changes with a clear decrease of amplitude at the E/O boundary at a depth of ~78 mbsf. Seismic data below ~100 ms TWT show interlayering of weak and strong reflector packages, including the Elmo horizon and the PETM, down to the basement at ~300 ms TWT. Both clay layers are characterized by strong amplitudes. The Elmo horizon at ~115 mbsf appears as a single distinct continuous reflector, whereas the PETM at ~139 mbsf appears as the first reflector of a package of several reflectors with strong amplitudes. With a drilling depth of 209 mbsf it was possible to recover all critical transitions, including the K/T boundary, which is characterized by a strong amplitude reflection close to the crystalline basement at a depth of ~195 mbsf.

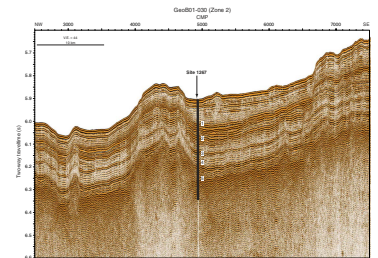
Site 1267

Site 1267, located on Profile GeoB01-030, is situated close to the edge of Angola Basin at a water depth of 4355 m (Fig. F5). The profile runs perpendicular to the ridge axis in a northwest-southeast direction. Sediment thickness in the northwest part of the profile is ~340 m. Site 1267 is located close to a basement high, which results in mostly parallel and undisturbed but inclined reflectors. Upper Maastrichtian sediments, which were the oldest sediments drilled during Leg 208, were reached at a drilling depth of 329 mbsf. The interval 0–150 ms TWT consists of Quaternary and Neogene sediments and includes a package of disturbed reflectors embedded with parallel reflectors with strong amplitudes. The Miocene *Bolivina* Acme is the first reflector of a package of stronger reflectors at ~111 mbsf. The E/O boundary at ~128 mbsf is a strong continuous reflector. In contrast to Site 1262, underlying reflectors also show high amplitudes. The Elmo horizon at ~179 mbsf is characterized by a continuous distinct reflector with strong amplitudes surrounded by sediments with lower amplitudes. The PETM at ~231 mbsf is embedded within a package of parallel reflectors with average amplitudes. At Site 1267, the K/T boundary was reached at a drilling depth of ~298 mbsf. The reflector representing the K/T boundary is located only ~30 m above the crystalline basement and shows strong amplitudes. Because of the proximity of the K/T reflector to basement with its rough surface, the reflector is not continuous along the profile.

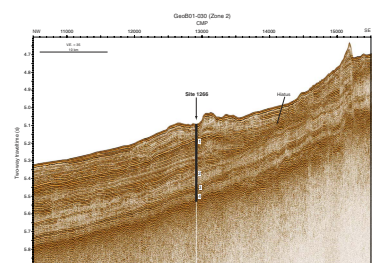
Site 1266

Site 1266, in a water depth of 3798 m, is also situated on Profile GeoB01-030 at the flank of the ridge (Fig. F6). It reaches upper Paleocene sediments at a drill depth of 334 mbsf. Sediments of Profile GeoB01-030 in the vicinity of Site 1266 along the flank of the ridge have a thickness of ~370 m, which is only slightly more than those at Site 1267. The northwest part of the profile is characterized by mostly undisturbed and parallel reflectors, but in the direction of the ridge with decreasing wa-

F5. Seismic Line GeoB01-030, Site 1267, p. 20.



F6. Seismic Line GeoB01-030, Site 1266, p. 21.



ter depth the pattern becomes more and more disturbed. Close to Site 1266 an unconformity occurs that results from a Neogene hiatus. Amplitudes of seismic reflectors at Site 1266 vary with depth, although only a few intervals with low amplitudes exist. The Miocene *Bolivina* Acme at ~115 mbsf is a continuous reflector with high amplitudes within a larger package of strong reflectors. The E/O boundary at ~207 mbsf is a transition from high amplitudes to a package of reflectors that are slightly disturbed and have lower amplitudes. The boundary is not as sharp as at Site 1262, for example (Fig. F4). The Elmo horizon at ~270 mbsf and the PETM at ~306 mbsf are parts of packages with strong amplitudes. The package including the PETM is the lowermost sediment package that overlies the crystalline basement. The package consists of disturbed high-amplitude reflectors.

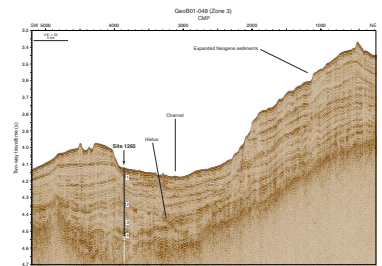
Site 1265

Site 1265 is located on Profile GeoB01-048, which is almost parallel to the axis of the ridge in a northeast-southwest direction (Fig. F7). The profile shows increasing sediment thickness up to ~450 m with decreasing water depth. Reflectors are mostly undisturbed and parallel except in a big channel structure in the center of the profile where Quaternary and Neogene sediments thin out. The reflectors of the flank of the channel are thinned out, probably because of nondeposition. Additionally, the disturbed sedimentation pattern of older sediments (e.g., Eocene) in the center of channel likely indicates changing current activities. Expanded Neogene sediments shown in the northeast part of Profile GeoB01-048 are part of a morphologic high in which the shallowest site, Site 1264 (see below), was drilled. The morphologic high is characterized by the thickest sediments sequence at Walvis Ridge (up to 450 m). Site 1265 was drilled at the edge of the channel, where Quaternary and Neogene sediments are thin and older sediments are not disturbed by proximity to the channel. At a water depth of 3060 m and a drilling depth of 321 mbsf, Site 1265 reaches upper Paleocene sediments. The Miocene *Bolivina* Acme event within the uppermost 100 ms TWT at ~88 mbsf is characterized by a strong continuous reflector that is disturbed or absent in the center of the large channel. The E/O boundary at ~192 mbsf is situated in the interval between ~200 and 300 ms TWT. The boundary is not as sharp at other sites, but still a small change from higher to lower amplitudes beneath is notable. The boundary is not continuous, especially in northwest direction, where sedimentation was possibly disturbed by variable current activities. The Elmo horizon at a depth of ~241 mbsf in the interval of ~300 to 400 ms TWT is not conspicuous because of only a small increase of the reflector amplitude. The PETM at ~315 mbsf is again part of the package with higher amplitudes but is not resolved as one continuous reflector.

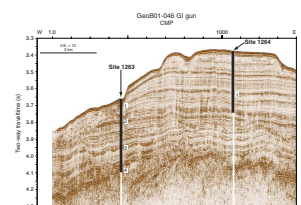
Sites 1263 and 1264

Sites 1263 and 1264, located on Profile GeoB01-046 (Fig. F8), were drilled close to the ridge flank where sediment column thickness varies from ~360 m at Site 1263 to ~450 m at Site 1264. Akin to Profile GeoB01-048 (Fig. F7), the profile shows an channel with thinned out reflectors at the flank and an expanded Quaternary and Neogene section. The western flank of the channel is not shown on the profile. The expanded section of Quaternary and Neogene sediments shown in the

F7. Seismic Line GeoB01-048, Site 1265, p. 22.



F8. Seismic Line GeoB01-046, Sites 1263 and 1264, p. 23.



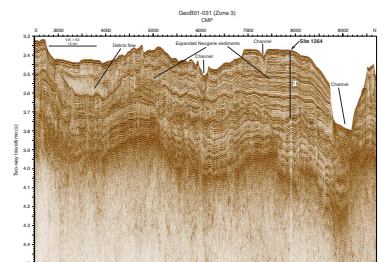
eastern part of Profile GeoB01-046 are part of the morphologic high, which also appears on Profile GeoB01-048.

Site 1263, at a water depth of 2717 m, was drilled into an apparent bottom water channel where Quaternary and Neogene sediments are absent or thin and thus Paleogene sediments are shallow in depth. The upper ~100 ms TWT represents thinned out Quaternary and Neogene sediment sequences. It includes the Miocene *Bolivina* Acme at ~44 mbsf, which appears as a continuous reflector with high amplitudes. The parallel to subparallel reflectors below ~100 to ~300 ms TWT show high amplitudes and good continuity. At ~100 mbsf the E/O boundary appears as a sequence of continuous reflectors with high amplitudes. Reflectors below ~300 ms TWT start to undulate with depth. This unit shows varying amplitudes and includes the Elmo event as a strong reflector at ~265 mbsf. The site reaches Paleocene sediments, including the PETM, which is surrounded by reflectors with high amplitudes at ~335 mbsf.

Site 1264 was drilled into an expanded section of Neogene sediments on the morphologic high close to the ridge flank. The location of the site is the crosspoint of Profiles GeoB01-046 (Fig. F8) and GeoB01-031 (Fig. F9). The morphologic high, illustrated on both profiles, is characterized by parallel layered sediment sequences. The sediments are disturbed by a slump or debris flow deposition shown in the south of Profile GeoB01-031 and smaller channels in the younger sediments in the north of the profile.

Site 1264, in a water depth of 2505 m, reaches Oligocene sediments at 282 mbsf. The parallel layered sediments represent a high-resolution data set of Quaternary and Neogene sediments with a pattern of varying strong and weak amplitudes in which the Miocene *Bolivina* Acme appears at ~159 mbsf as a continuous reflector with strong amplitudes.

F9. Seismic Line GeoB01-031, Site 1264, p. 24.



DISCUSSION

Seismic Characterization of Target Horizons

The main objective of the project is stratigraphy and correlation between seismic and well data, which is based on pattern recognition of reflector sequences in the first place. Identification of the critical transition in the entire survey area is of great importance for this approach. As demonstrated above, we can identify the critical transitions in the seismic data at the locations of the Leg 208 drill sites, demonstrating that our relatively simple event modeling is sufficient for this task. Seismic characteristics for each target horizon at Leg 208 drill sites were studied.

Miocene *Bolivina* Acme Event

The Miocene *Bolivina* Acme Event is a continuous reflector with strong amplitudes within Neogene sediments. Depending on the thickness of the Neogene sequences, it is surrounded by sediments with lower amplitudes (Sites 1264 and 1265) or is part of a package with strong amplitudes (Sites 1262, 1266, and 1267).

E/O Boundary

The E/O boundary in core samples is marked by a step increase in magnetic susceptibility (Shipboard Scientific Party, 2003), which sug-

gests a change of the physical properties of the sediments. In seismic data the E/O boundary is represented by a sharp transition from a package of sediments imaged as reflectors with strong amplitudes to a package of sediments imaged with lower amplitudes at all sites except at Site 1266, where possibly synsedimentary slumping during the Oligocene disturbed the sedimentation pattern.

Elmo Horizon

The Elmo horizon is represented as a strong, continuous, mostly isolated reflector surrounded by sediments with lower amplitudes. The Elmo horizon, which is characterized by a 30- to 50-cm-thick layer with 10% higher density than the surrounding sediments, includes a drop in calcium carbonate content (Shipboard Scientific Party, 2003). It has a strong impedance contrast resulting in a continuous reflector with high amplitudes.

PETM

The PETM is also characterized by low carbonate content and 10% higher density. Because of a surrounding sediment with strong amplitudes, the 50- to 80-cm-thick clay layer (Shipboard Scientific Party, 2003) cannot be resolved as an individual reflector with GI gun data. Therefore, the PETM is not imaged as an individual reflector, but sediments at the depth of the PETM are characterized by strong amplitudes at all sites except for Site 1264, which was not drilled to PETM depth.

K/T Boundary

The K/T boundary at Sites 1262 and 1267 occurs as the first reflector of a reflector package with strong amplitudes and a sharp transition immediately above basement. The basal contact of this clay layer is also sharply defined by an increase in magnetic susceptibility data.

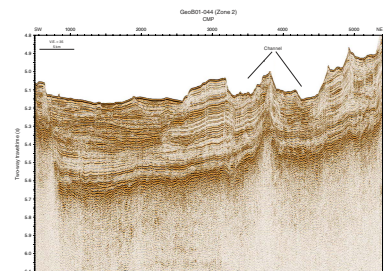
Sedimentary Features on Outer Walvis Ridge

Most of the sediments at Walvis Ridge are characterized by undisturbed sediment sequences, but based on changing deposition conditions, varying basement structures, and/or influences of bottom water currents, it is possible to separate the study area into three zones (Fig. F1). Zone 1 covers the northwestern part of the study area, that is the beginning of Angola Basin. Basement is partly faulted, as shown on profiles running parallel to the axis of the ridge, which results in a rough basement topography (Fig. F4) with small basins filled with pelagic sediments. These sediments are generally undisturbed except some debris flow or slump structures in the younger sections. The shallow-dipping basement parallel to the flank of the ridge is mostly not faulted. Zone 1 is characterized by the smallest sediment thickness of ~150 to 200 m.

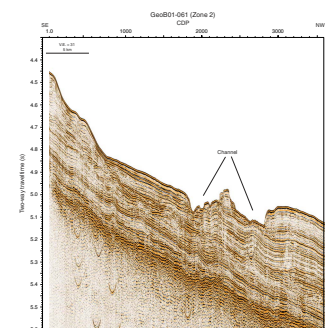
Zone 2 covers the flank of the ridge (Fig. F1). Sediment thickness increases toward the ridge axis. Basement is smoother compared to Zone 1, which probably indicates less tectonic activity. The sedimentation pattern is more disturbed than in Zone 1 because of the flank's slope of 0.7° (Figs. F10, F11). A few channel structures at the flank of the ridge appear in a small part of Zone 2 (Figs. F1, F10, F11).

In Zone 3, sediment thickness reaches 450 m. Adjacent to some smaller channels with a width of 1–2 km (Fig. F9), there are larger chan-

F10. Seismic Line GeoB01-044, p. 25.



F11. Seismic Line GeoB01-061, p. 26.



nel structures with widths up to some tens of kilometers, indicating a large zone influenced by bottom water currents (Fig. F7). The thickness of Neogene sediments is significantly decreased in this area, whereas older sediment packages show a similar thickness as the surrounding areas. Hence, confined bottom currents occurred mainly in the Neogene. These changing deposition conditions offered the possibility to drill Sites 1263, 1264, and 1265 within a few kilometers with varying thickness of Neogene sediments (Figs. F7, F8, F9). No major faults were identified along the axis of the ridge, suggesting a mostly undisturbed sedimentary sequence.

CONCLUSIONS

The collected seismic data from *Meteor* Expedition M49/1 are of high quality, allowing excellent site selection for Leg 208 drilling locations. Correlation of seismic data with borehole data was accomplished by calculating synthetic seismograms using GRA density measurements of the cores and an averaged velocity model. This method allowed “simple” event modeling to assign ages to the seismic reflectors and to identify key horizons/boundaries like the E/O and the K/T boundaries or the Miocene *Bolivina* Acme, Elmo, and PETM horizons. Characteristics of these target horizons show similar properties at different sites, which indicates the regional distribution of each.

Sediment thickness of the study area increases from Angola Basin (~150 m) to the axis of Walvis Ridge (~450 m). Because of the changing deposition conditions, the Leg 208 study area is separated into three zones. Zone 1 is characterized by basement faulting that results in formation of a small basins at the beginning of Angola Basin. Basins are filled up with mostly undisturbed pelagic sediments, whereas younger sediments in these basins partly constitute debris flow or slump deposits. Zone 2 on the flank of the ridge is characterized by an increasing sediment thickness and an area with several smaller channel structures indicating bottom water currents. Zone 3, at the axis of the ridge, shows the most varying sedimentation pattern. Among some expanded Neogene and Quaternary sections with the largest sediment thickness of the study area, several erosive channels of variable width occur, suggesting strong bottom current activities.

ACKNOWLEDGMENTS

We are grateful for the support of the captain and the crew members as well as all cruise members of *Meteor* Cruise M49/1 for their help during the expedition. We also want to thank the Scientific Shipboard Party of the ODP Leg 208, who did a great job, especially Jim Zachos for his comments and help during this study. This research used samples and/or data provided by the Ocean Drilling Program (ODP). ODP is funded by the U.S. National Science Foundation (NSF) and participating countries under management of Joint Oceanographic Institutions (JOI), Inc. This research was funded by Deutsche Forschungsgemeinschaft, Grant Sp 296/24-1, “Sedimentation processes on Walvis Ridge—correlation of high resolution seismic records with ODP Leg 208 physical properties data.”

REFERENCES

- Adcock, S., 1993. In search of the well tie: what if I don't have a sonic log? *Leading Edge*, 12(12):1161–1164. doi:10.1190/1.1436929
- Arhan, M., Mercier, H., and Park, Y.-H., 2003. On the deep water circulation of the eastern South Atlantic Ocean. *Deep-Sea Res., Part I*, 50(7):889–916. doi:10.1016/S0967-0637(03)00072-4
- Badley, M.E., 1985. *Practical Seismic Interpretation*: Englewood Cliffs, NJ (Prentice Hall).
- Breitzke, M., 2000. Physical properties of marine sediments. In Schulz, H.D., and Zabel, M. (Eds.), *Marine Geochemistry*: Berlin (Springer Verlag), 29–72.
- Hamilton, E.L., 1976. Variations of density and porosity with depth in deep sea sediments. *J. Sediment. Petrol.*, 46:280–300.
- Kaiho, K., Arinobu, T., Ishiwatari, R., Morgans, H.E.G., Okada, H., Takeda, N., Tazaki, K., Zhou, G., Kajiwaru, Y., Matsumoto, R., Hirai, A., Niitsuma, N., and Wada, H., 1996. Latest Paleocene benthic foraminiferal extinction and environmental changes at Tawanui, New Zealand. *Paleoceanography*, 11(4):447–466. doi:10.1029/96PA01021
- Mendel, J.M., Nahi, N.E., and Chan, M., 1979. Synthetic seismograms using the state-space approach. *Geophysics*, 44(5):880–895. doi:10.1190/1.1440983
- Moore, T.C., Jr., Rabinowitz, P.D., et al., 1984. *Init. Repts. DSDP*, 74: Washington, D.C. (U.S. Govt. Printing Office).
- Mosher, D.C., Mayer, L.A., Shipley, T.H., Winterer, E.L., Hagen, R.A., Marsters, J.C., Bassinot, F., Wilkens, R.H., and Lyle, M., 1993. Seismic stratigraphy of the Ontong Java Plateau. In Berger, W.H., Kroenke, L.W., Mayer, L.A., et al., *Proc. ODP, Sci. Results*, 130: College Station, TX (Ocean Drilling Program), 33–49. doi:10.2973/odp.proc.sr.130.047.1993
- Rabinowitz, P.D., and Simpson, E.S.W., 1984. Geophysical site survey results on the Walvis Ridge. In Moore, T.C., Jr., Rabinowitz, P.D., et al., *Init. Repts. DSDP*, 74: Washington (U.S. Government Printing Office), 795–825.
- Ricker, N., 1953. The form and laws of propagation of seismic wavelets. *Geophysics*, 18(1):10–40. doi:10.1190/1.1437843
- Rohr, K.M.M., and Gröschel-Becker, H., 1994. Correlation of well logs, physical properties, and surface seismic reflection data, Middle Valley, Juan de Fuca Ridge. In Mottl, M.J., Davis, E.E., Fisher, A.T., and Slack, J.F. (Eds.), *Proc. ODP, Sci. Results*, 139: College Station, TX (Ocean Drilling Program), 585–596. doi:10.2973/odp.proc.sr.139.257.1994
- Shipboard Scientific Party, 2003. Leg 208 Preliminary Report. *ODP Prelim. Rpt.*, 108 [Online]. Available from World Wide Web: <http://www-odp.tamu.edu/publications/prelim/208_prel/208PREL.PDF>.
- Smart, C.W., and Murray, J.W., 1994. An early Miocene Atlantic-wide foraminiferal/palaeoceanographic event. *Palaeogeogr., Palaeoclimatol., Palaeoecol.*, 108(1–2):139–148. doi:10.1016/0031-0182(94)90026-4
- Weber, M.E., Niessen, F., Kuhn, G., and Wiedicke, M., 1997. Calibration and application of marine sedimentary physical properties using a multi-sensor core logger. *Mar. Geol.*, 136(3–4):151–172. doi:10.1016/S0025-3227(96)00071-0
- White, R.E., and Hu, T., 1998. How accurate can a well tie be? *Leading Edge*, 17(8):1065–1071. doi:10.1190/1.1438091
- Zachos, J.C., Kroon, D., Blum, P., et al., 2004. *Proc. ODP, Init. Repts.*, 208: College Station, TX (Ocean Drilling Program). doi:10.2973/odp.proc.ir.208.2004
- Zühlsdorff, L., and Spiess, V., 2001. Modeling seismic reflection patterns from Ocean Drilling Program Leg 168 core density logs: insight into lateral variations in physical properties and sediment input at the eastern flank of the Juan de Fuca Ridge. *J. Geophys. Res.*, 106(B8):16119–16134. doi:10.1029/2001JB900005

Figure F1. Seismic presite survey ODP Leg 208. ODP = Ocean Drilling Program, DSDP = Deep Sea Drilling Project.

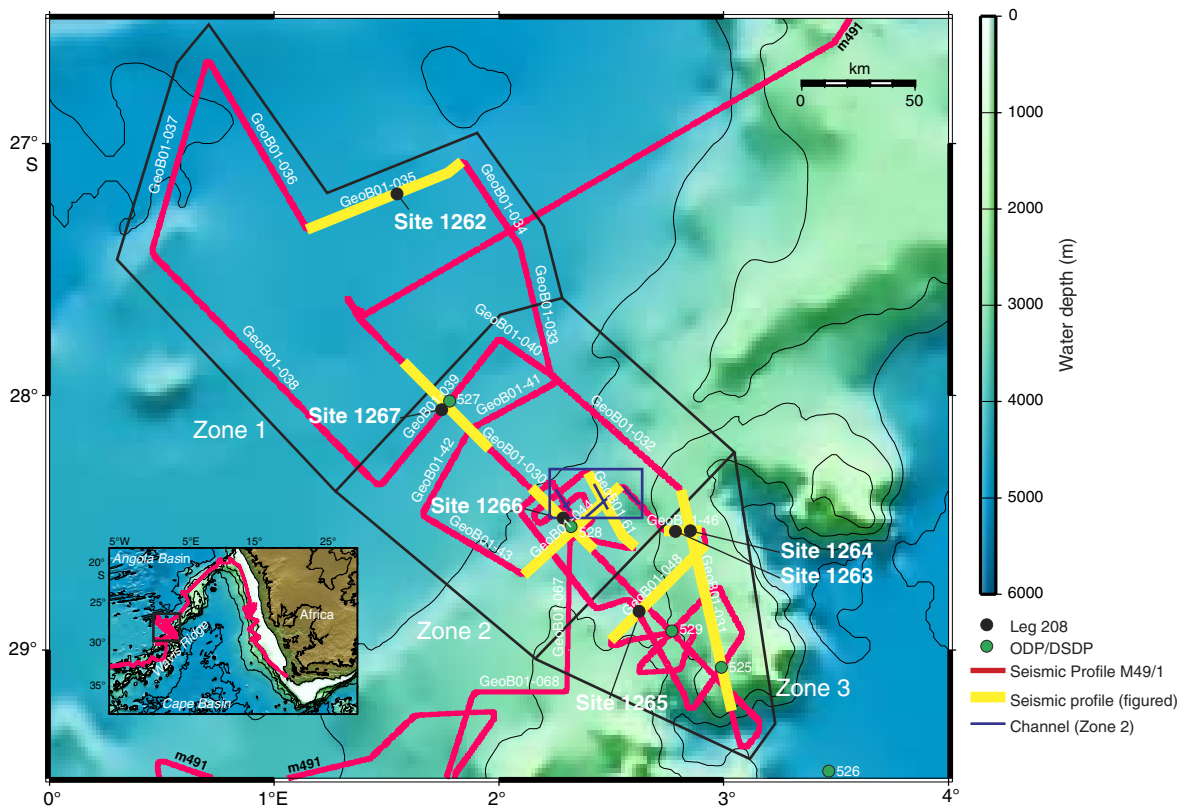


Figure F2. GRA density, velocity, reflection coefficients, and synthetic seismograms. A. Site 1262. GRA density constructed using Splice Tables and data from Holes 1262A, 1262B, 1262C, and 1262D for A, Holes 1264A, 1264B, and 1264C for B, Holes 1266A, 1266B and 1266C for C, and Holes 1267A and 1267B for D. Red line = regression line used for conversion from a depth scale to a timescale. Ricker wavelet with 150 Hz was used for synthetic seismograms. (Continued on next three pages.)

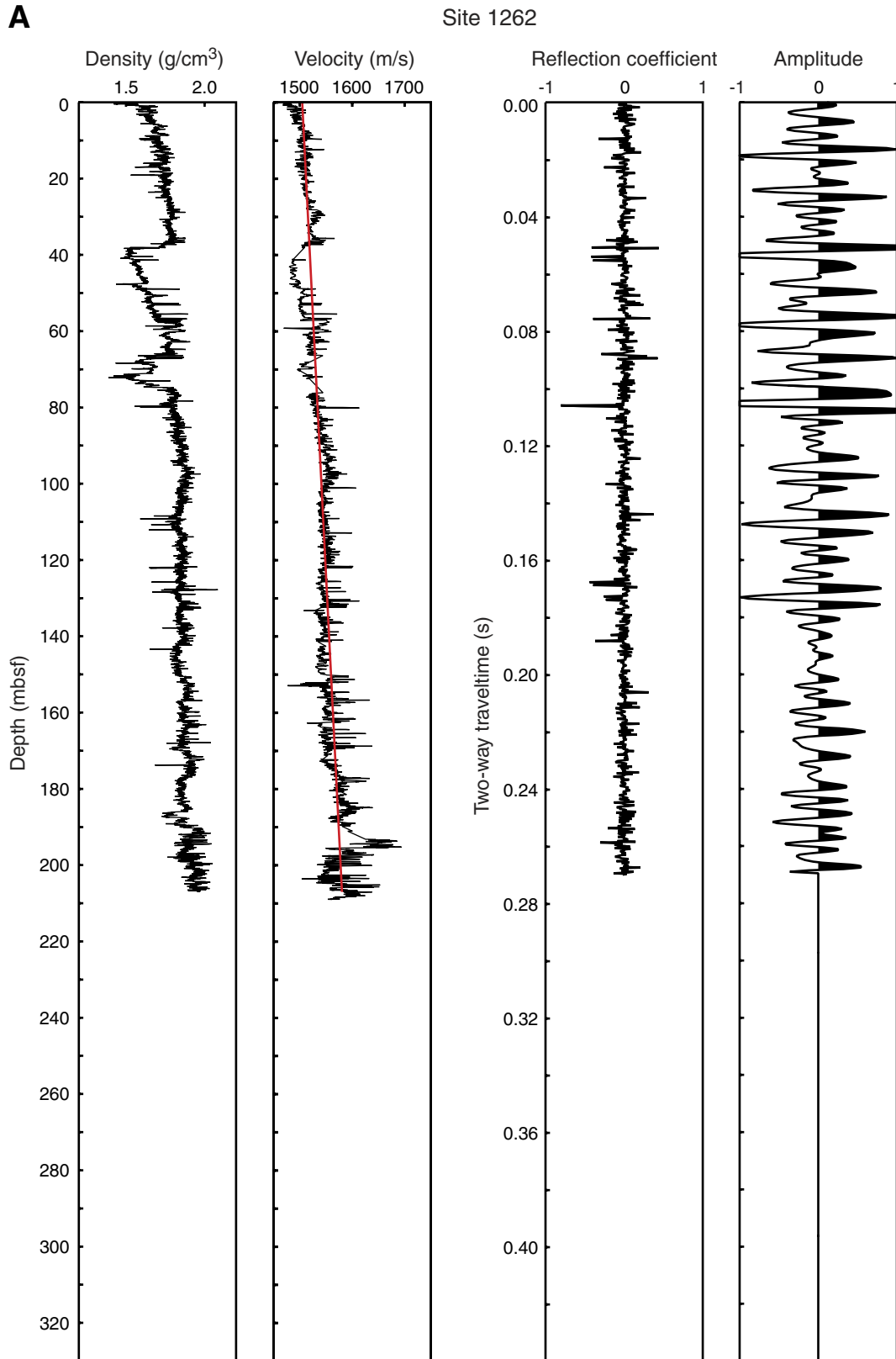


Figure F2 (continued). B. Site 1264. (Continued on next page.)

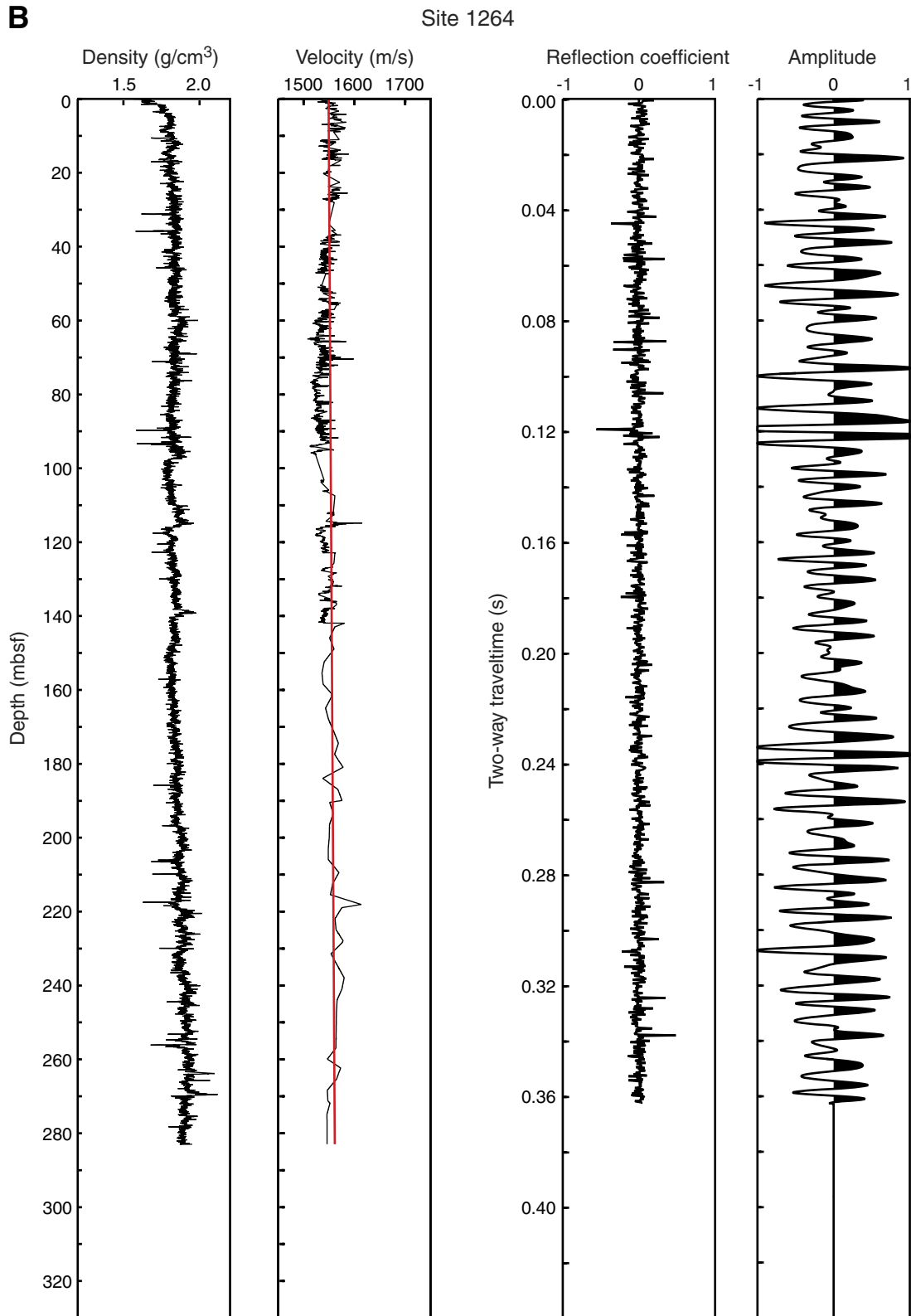


Figure F2 (continued). C. Site 1266. (Continued on next page.)

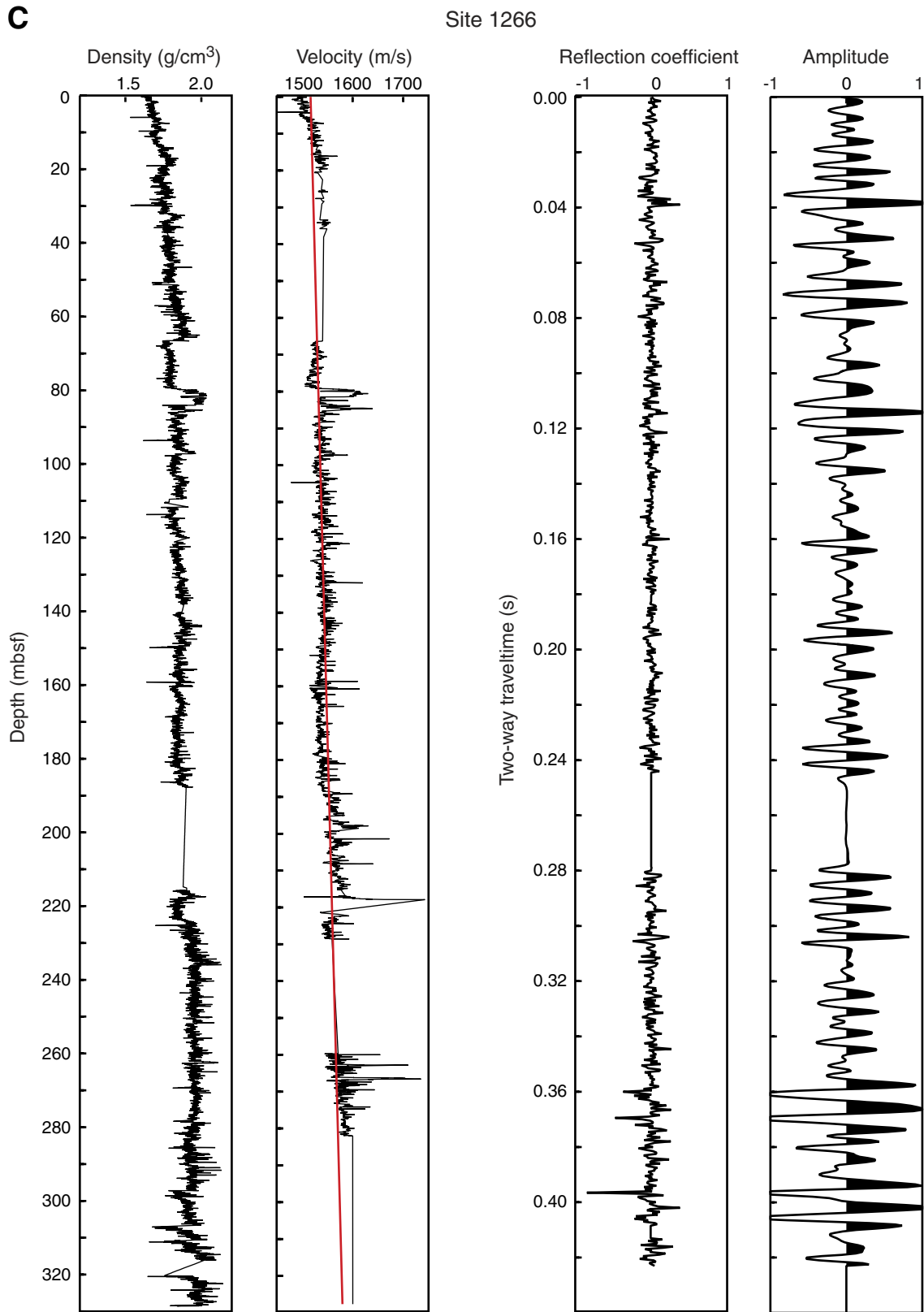


Figure F2 (continued). D. Site 1267.

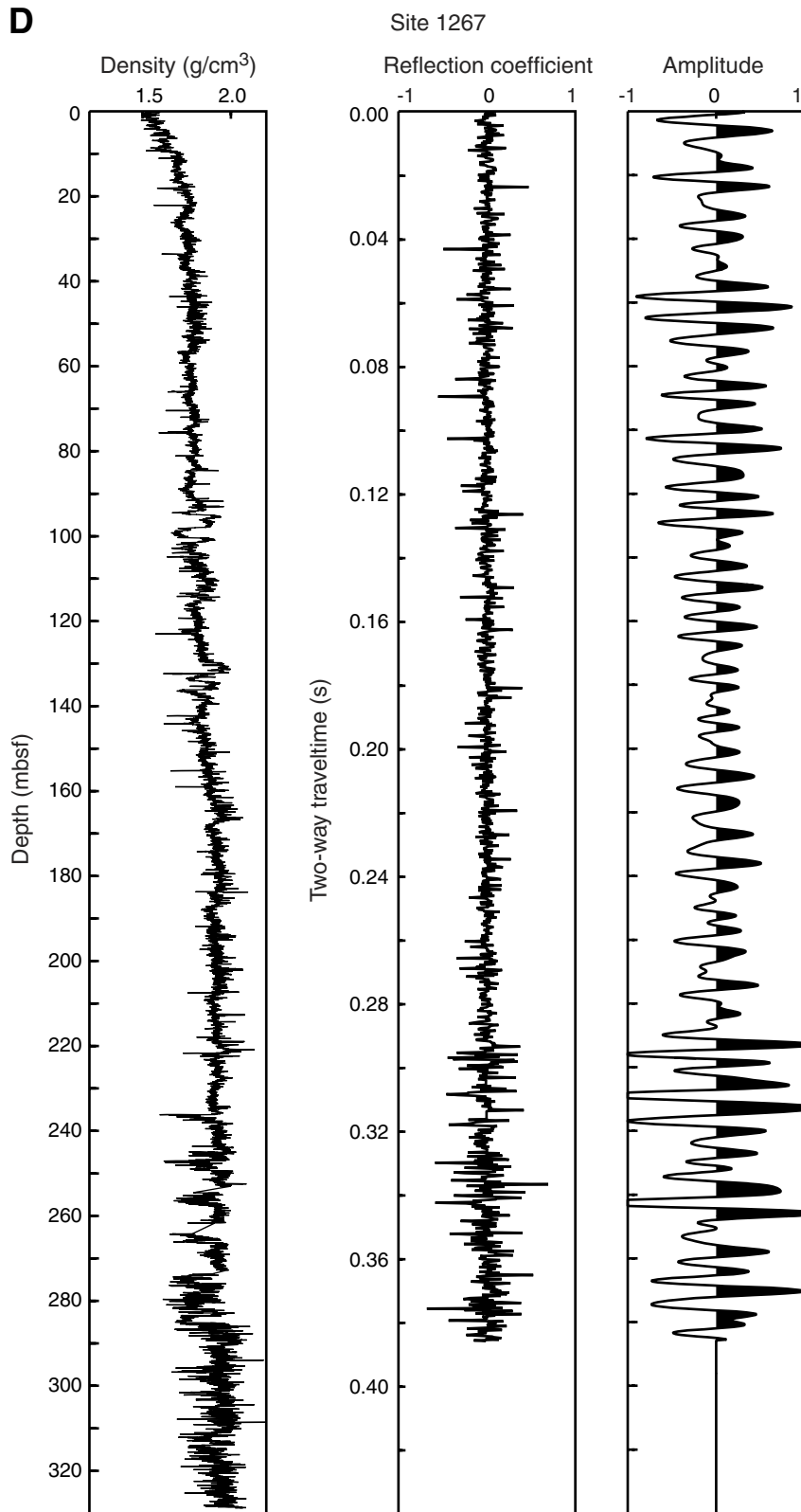


Figure F3. Correlation of synthetic seismograms with the seismic data for Sites (A) 1262, (B) 1264, (C) 1266, and (D) 1267. Horizons: 1 = Miocene *Bolivina* Acme, 2 = E/O boundary, 3 = Elmo horizon, 4 = PETM, 5 = K/T boundary. CMP = common midpoint, GI = generator injector.

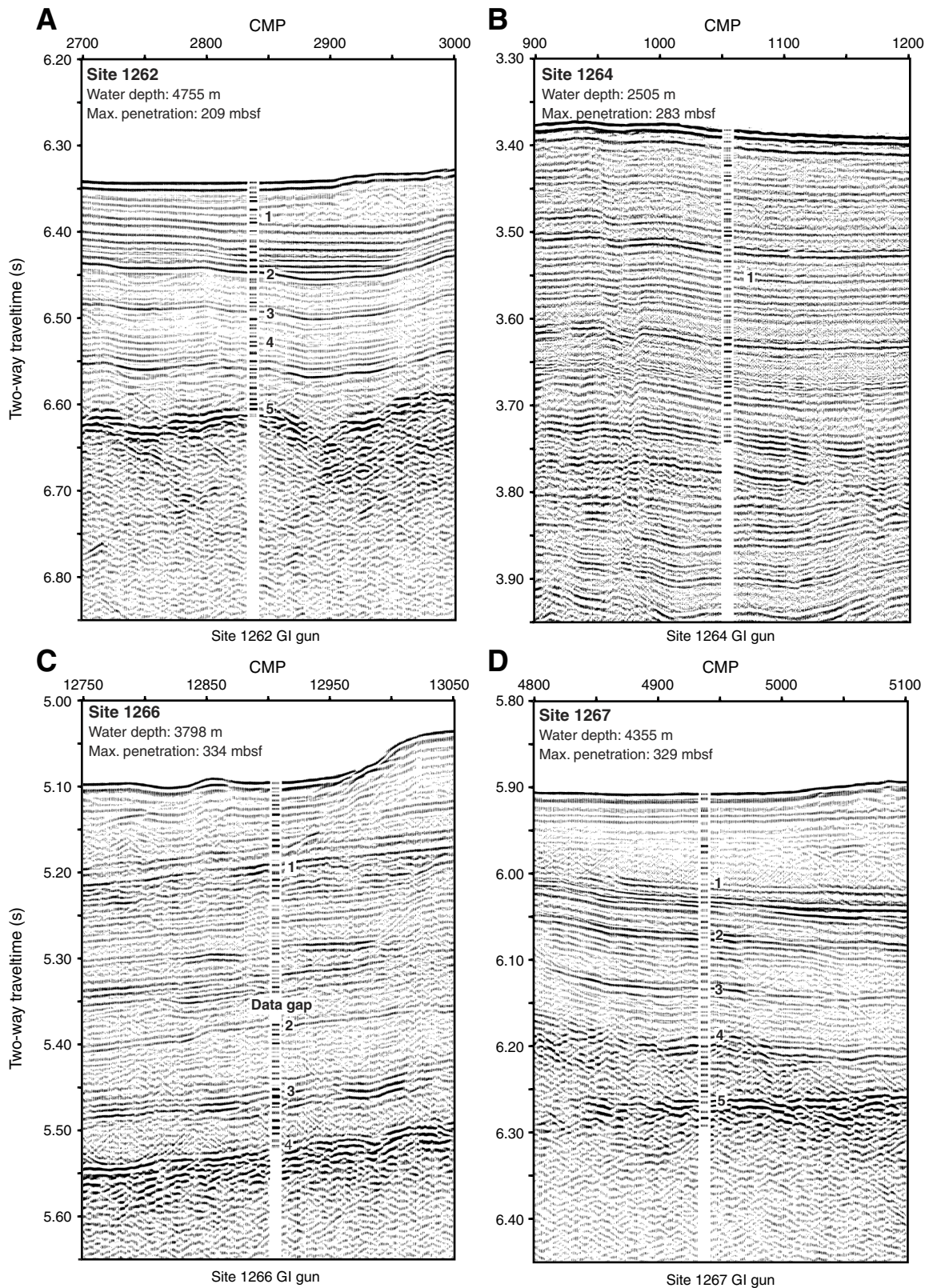


Figure F4. Seismic Line GeoB01-035, Site 1262. Horizons: 1 = Miocene *Bolivina* Acme, 2 = E/O boundary, 3 = Elmo horizon, 4 = PETM, 5 = K/T boundary. V.E. = vertical exaggeration.

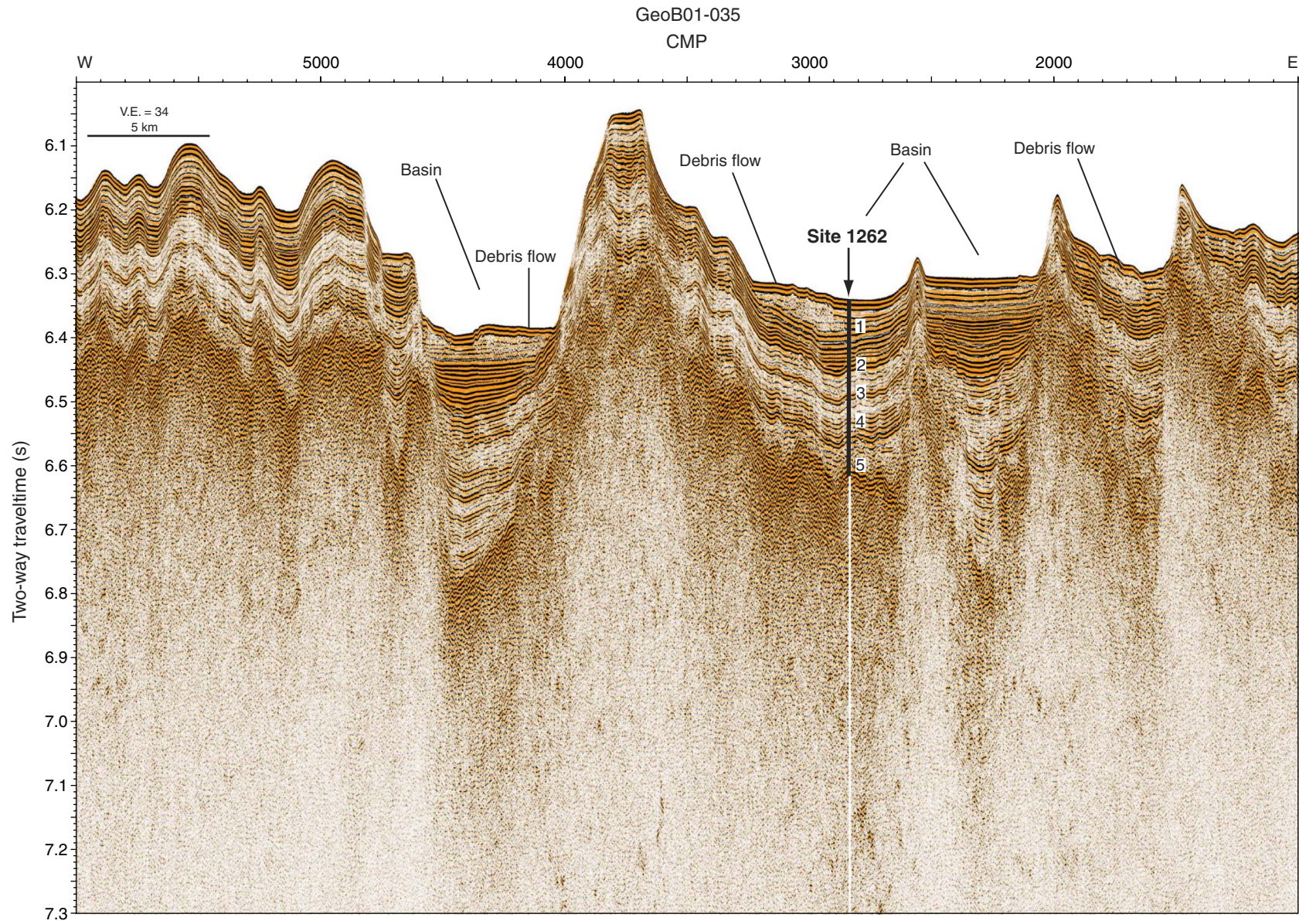


Figure F5. Seismic Line GeoB01-030, Site 1267. Horizons: 1 = Miocene *Bolivina* Acme, 2 = E/O boundary, 3 = Elmo horizon, 4 = PETM, 5 = K/T boundary. V.E. = vertical exaggeration.

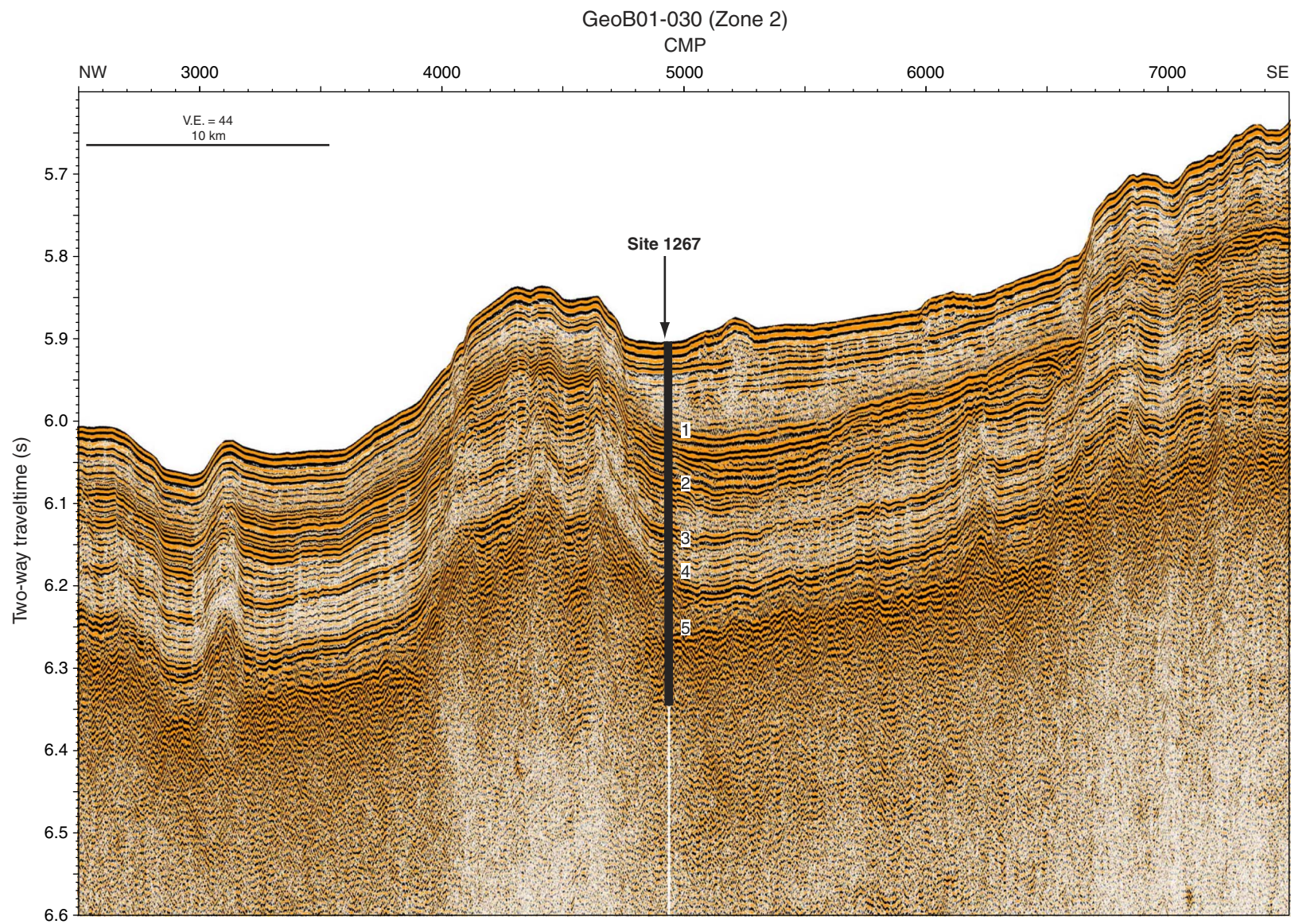


Figure F6. Seismic Line GeoB01-030, Site 1266. Horizons: 1 = Miocene *Bolivina* Acme, 2 = E/O boundary, 3 = Elmo horizon, 4 = PETM. V.E. = vertical exaggeration.

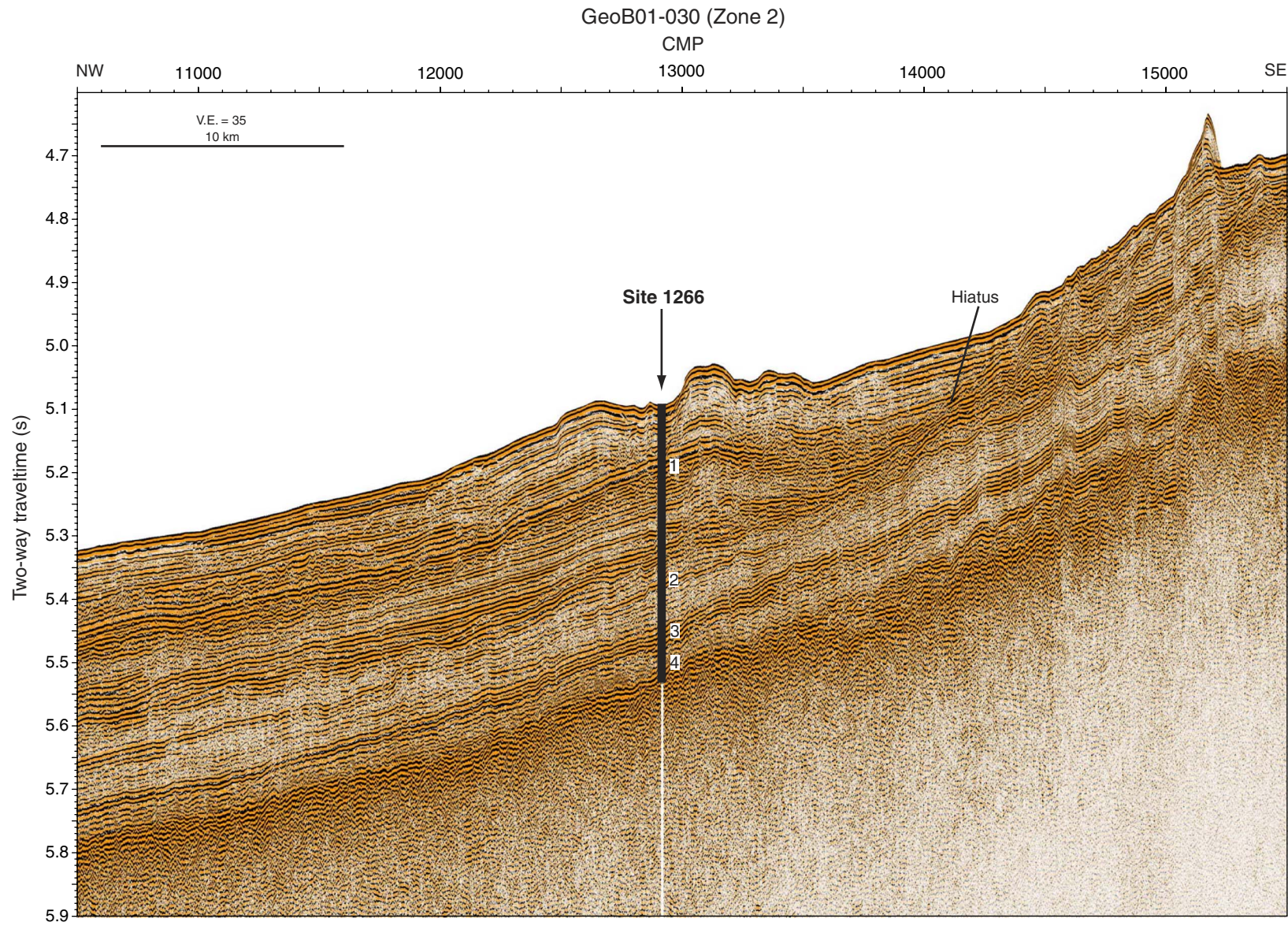


Figure F7. Seismic Line GeoB01-048, Site 1265. Horizons: 1 = Miocene *Bolivina* Acme, 2 = E/O boundary, 3 = Elmo horizon, 4 = PETM. V.E. = vertical exaggeration.

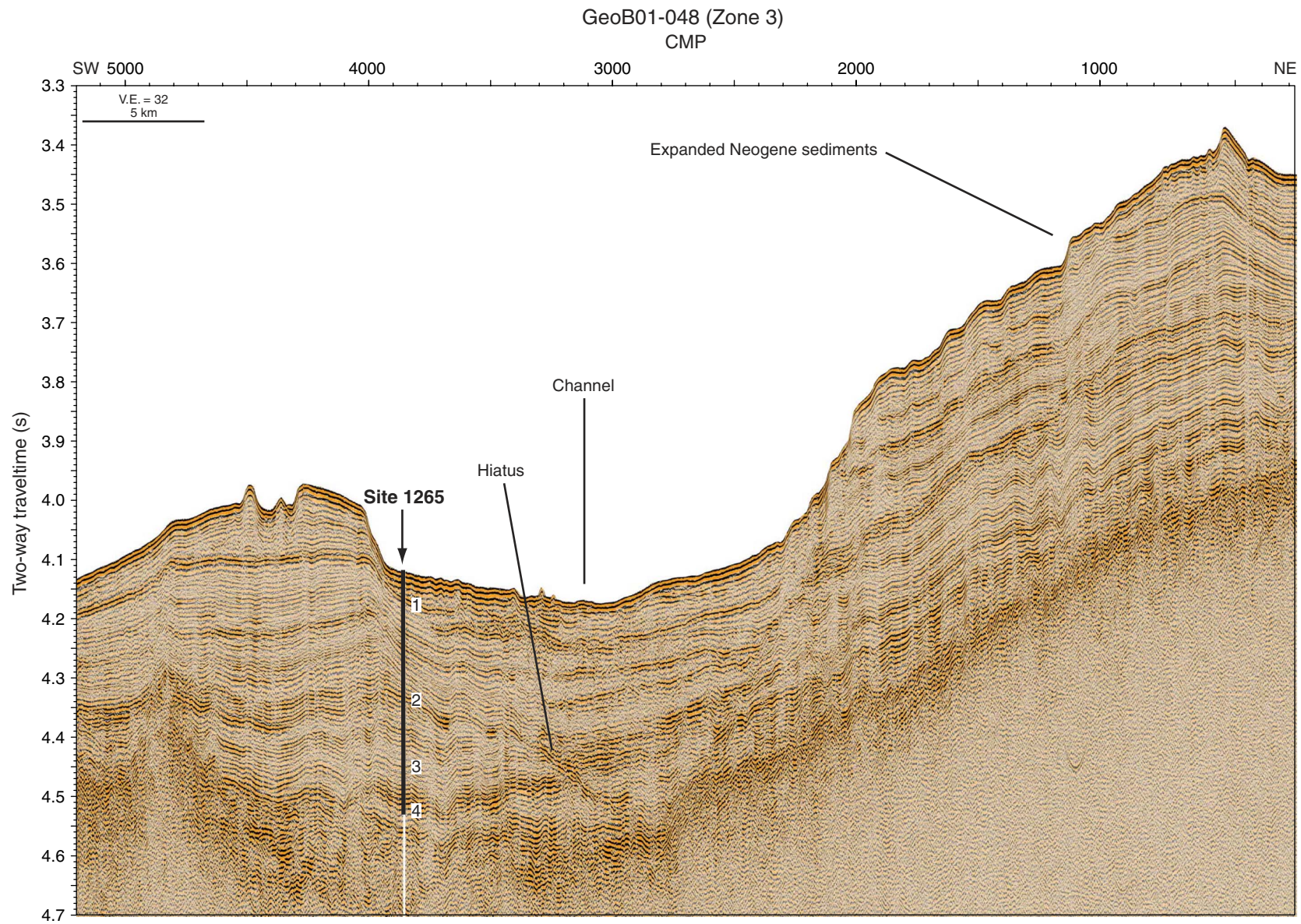


Figure F8. Seismic Line GeoB01-046, Sites 1263 and 1264. Horizons: 1 = Miocene *Bolivina* Acme, 2 = E/O boundary, 3 = Elmo horizon, 4 = PETM. V.E. = vertical exaggeration.

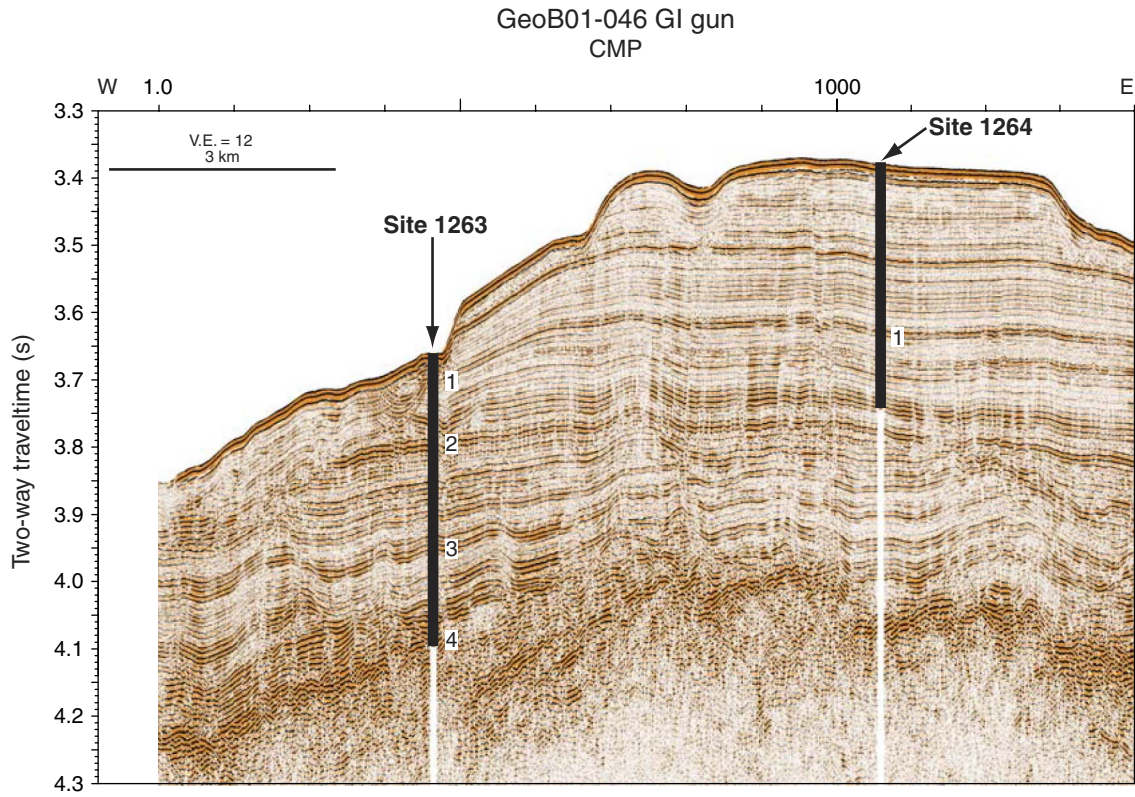


Figure F9. Seismic Line GeoB01-031, Site 1264. Horizon: 1 = Miocene *Bolivina* Acme. V.E. = vertical exaggeration.

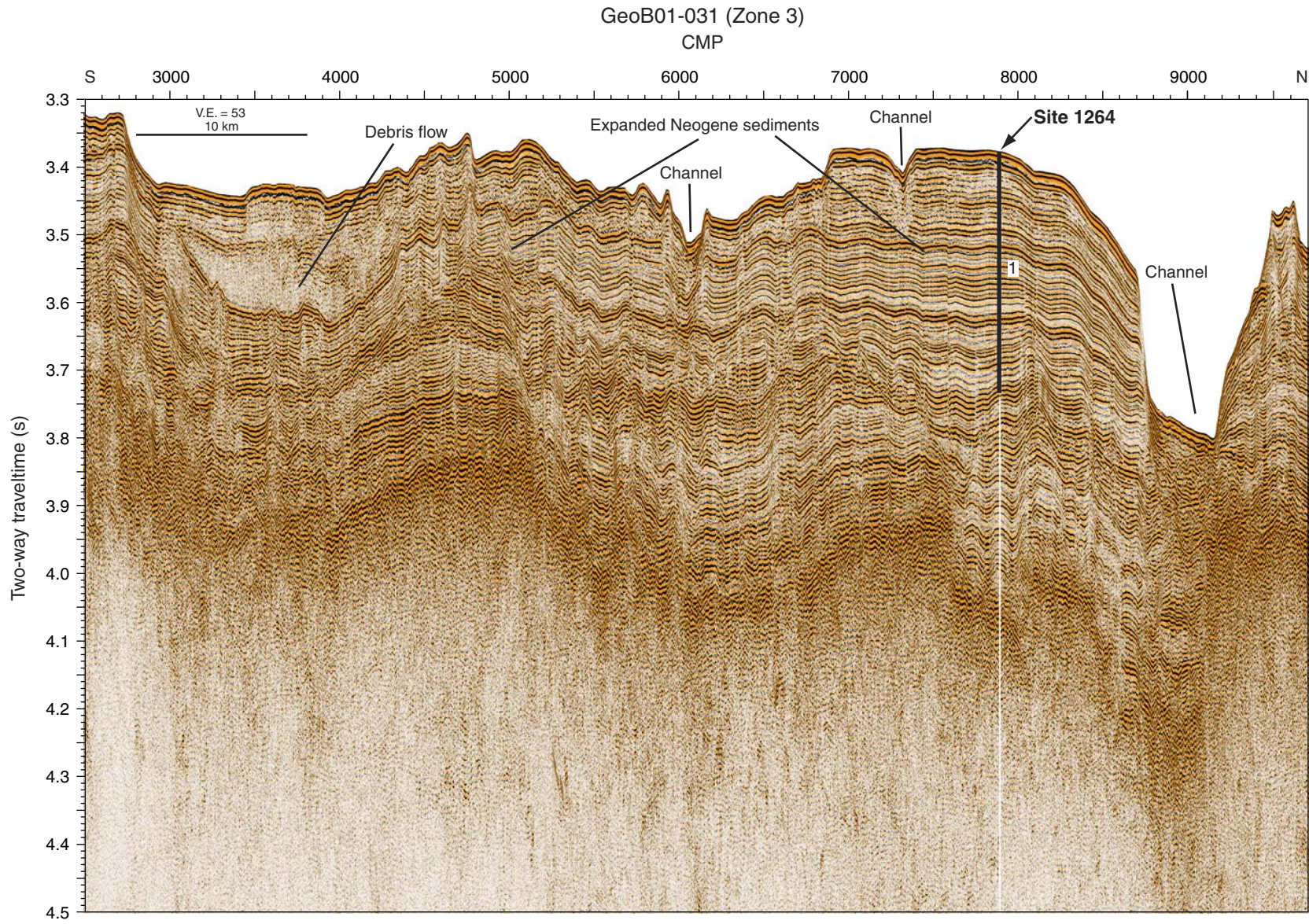


Figure F10. Seismic Line GeoB01-044. V.E. = vertical exaggeration.

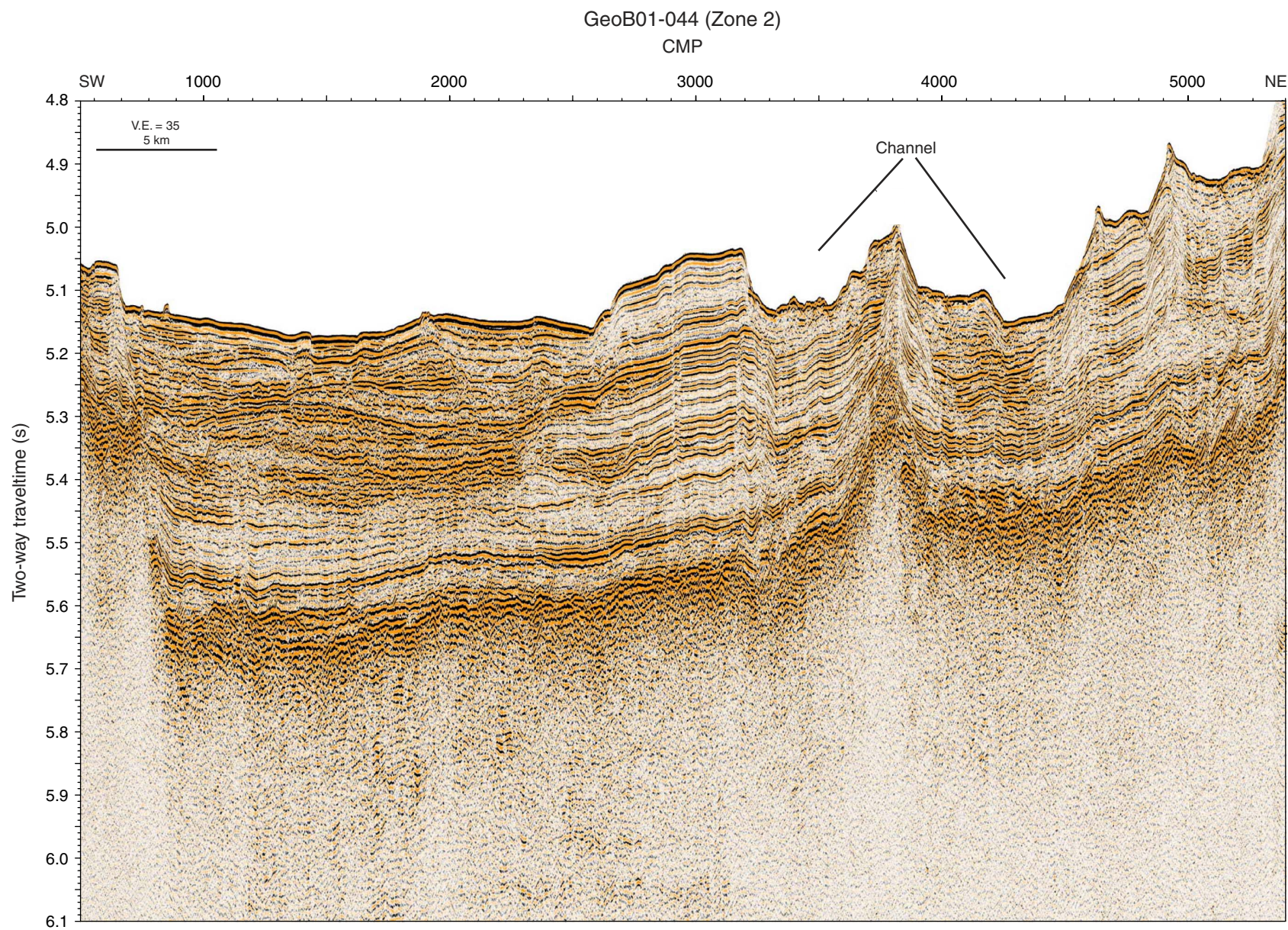


Figure F11. Seismic Line GeoB01-061. V.E. = vertical exaggeration.

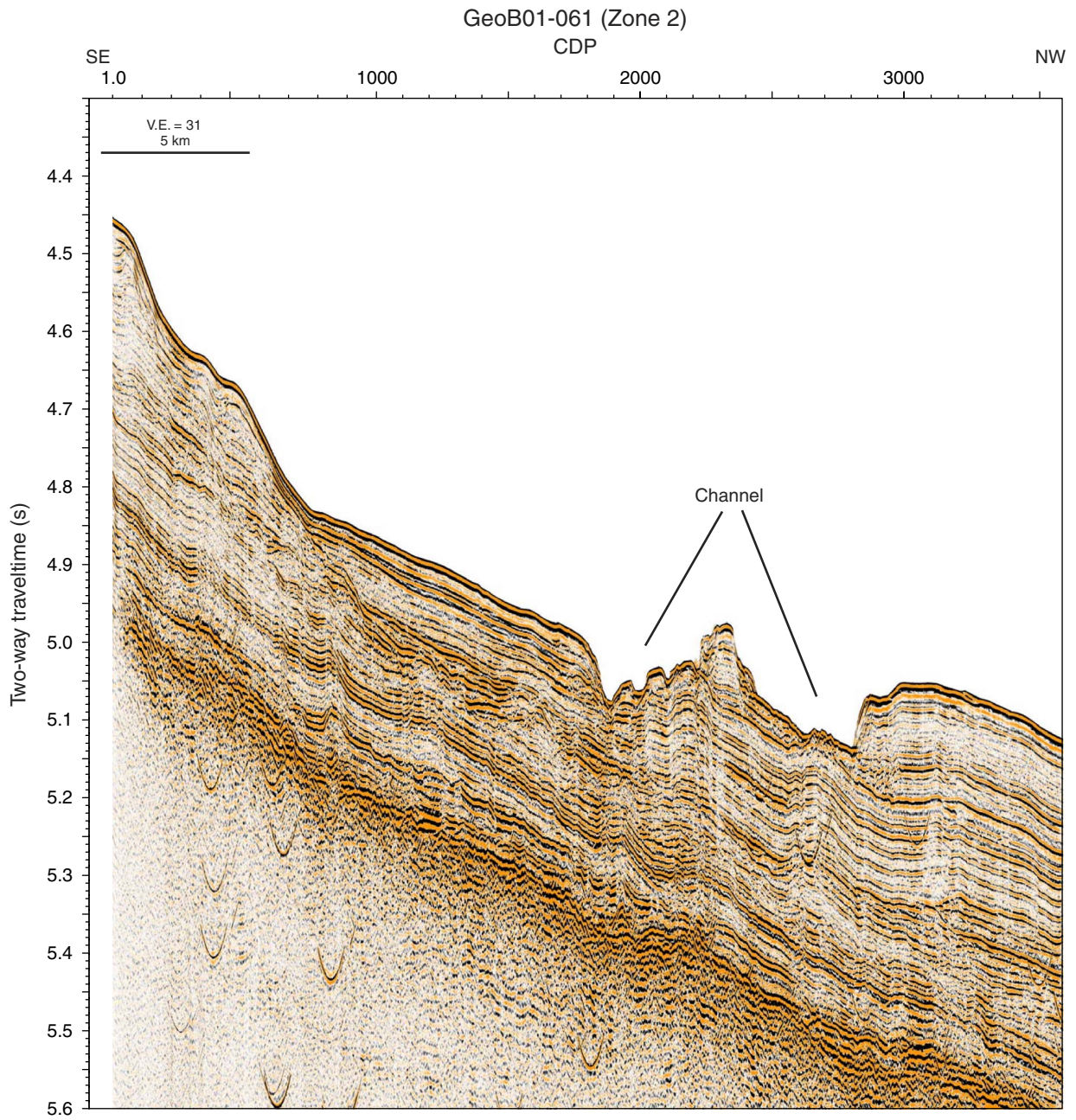


Table T1. Depth of target horizons at each site of Leg 208.

	Depth (mbsf)					
	Site 1262	Site 1263	Site 1264	Site 1265	Site 1266	Site 1267
Miocene <i>Bolivina</i> Acme	53	44	159	88	115	111
E/O boundary	78	100	—	192	207	128
Elmo horizon	115	265	—	241	270	179
PETM	139	335	—	315	306	231
K/T boundary	195	—	—	—	—	298

Notes: Depths calculated using velocity models of synthetic seismograms and traveltimes of seismic data. For Sites 1263 and 1265, a velocity model using a linear regression line was assumed. — = not identified on seismogram.